

Y-Ba-Cu-O SUPERCONDUCTING/GaAs SEMICONDUCTING HYBRID CIRCUITS
FOR MICROWAVE APPLICATIONS

K. B. Bhasin*, S. S. Toncich*, C. M. Chorey**, N. J. Rohrer*** and
G.J. Valco***

* National Aeronautics and Space Administration
Lewis Research Center, Cleveland, Ohio 44135

** Sverdrup Technology, Brook Park, Ohio 44142

*** Department of Electrical Engineering
Ohio State University, Columbus, Ohio 43210

ABSTRACT

We have combined a two pole superconducting bandpass filter with a packaged GaAs low noise amplifier, and have designed, fabricated, and tested a superconducting X-band oscillator. Both circuits have been compared to normal metal circuits at 77K. This paper presents the results of these experiments, technical issues, and potential applications.

INTRODUCTION

Before the discovery of high temperature superconducting (HTS) materials, the integration of low-Tc superconductors with semiconducting devices was not feasible since many semiconducting devices experience carrier freeze-out below 10K. Demonstrations of HTS passive microwave components operating at liquid nitrogen (77K) temperatures [1,2] has enhanced the feasibility of integrating HTS passive components with semiconductors to achieve high performance microwave systems [3]. GaAs and heterostructure microwave semiconducting devices make strong candidates for integration since they have much lower noise figures at 77K [4,5] than at 300K, while the operating temperature of 77K also avoids the problem of carrier freeze-out. To achieve the maximum benefit of HTS materials the level of integration between passive and active elements must be increased to the point where entire systems can operate reliably at liquid nitrogen temperatures for extended periods of time.

Integration of passive HTS devices with semiconductor devices can be achieved from the discrete component level up to the system level. Such a progression is shown in Figure 1. Levels 1 and 2 are now feasible due to the demonstration of high Tc superconducting microwave devices. Level 3 work is in the early stages at the present time. To determine the

performance advantages at the subsystem level, we have combined a two pole superconducting bandpass filter with a packaged GaAs low noise amplifier (LNA), and compared its performance with a gold filter/LNA hybrid circuit down to 35K. At the circuit level, we have designed, fabricated, and tested an X-band hybrid superconducting/GaAs oscillator on a single lanthanum aluminate substrate, where a high Q superconducting resonator is used for stabilization of the oscillator. High quality Y-Ba-Cu-O (YBCO) superconducting films were used in both experiments.

BPF/LNA HYBRID CIRCUIT

Several two-pole bandpass filter were designed with a 2.5 percent bandwidth, 0.5 dB passband ripple, and 7.5 GHz center frequency. The filters were fabricated using laser ablated YBCO superconducting films (approx. 5000Å) on a 0.01 inch lanthanum aluminate substrate. Gold film deposited by E-beam evaporation on the opposite side of the substrates formed ground planes for the circuits. An identical filter using gold film for the microstrip was also fabricated.

The LNA selected was an Avantek PGM 11421 with a specified bandwidth of 4 to 11 GHz, a gain of 8.0 dB, and a noise figure of 2.5 dB. A diagram of the hybrid is shown in Figure 2. The devices were connected by 0.010 inch gold bond wires to a 50 ohm microstrip line that was fabricated on a 0.01 inch thick Duroid ($\epsilon_r=2.3$) substrate. The hybrid was mounted on a brass test fixture using a conductive epoxy. SMA female flange connectors were used for the microstrip to coax transition.

All cryogenic measurements were made inside a closed cycle cryostat which has semi-rigid coaxial cables providing a connection between the

two temperature environments. An HP 8510B automatic network analyzer (ANA) was used to measure insertion gain or loss. A full two port calibration was performed inside the cryostat so as to move the reference planes of the ANA to the ends of these cables. Since this experiment is concerned only with relative changes in system performance, a two port cal was chosen over a TRL or LRL, that would have moved the reference planes of the ANA onto the test fixture. Noise figure measurements were made on a HP8970A noise figure meter, with loss compensation used to account for the test fixture's contribution to the system noise figure.

The LNA and filters were tested individually to determine their gain or loss and noise figures at $T=300K$ and $77K$. The HTS filter showed a significantly smaller insertion loss than the gold filter at $77K$, due to the near elimination of conductor loss in the YBCO film compared to the gold conductor. Most of the HTS filter loss is due to the gold ground plane; if it were replaced with HTS material the insertion loss would be nearly eliminated. At $77K$ the gold hybrid shows a noise figure improvement of 3.5 dB compared to $300K$, while the HTS hybrid shows a 5.5 dB improvement compared to gold at $300K$. These results are shown in Figure 3. The gain of the HTS hybrid is greater than the gold hybrid due to lower insertion loss in the HTS filter [6].

SUPERCONDUCTING OSCILLATOR

The high "Q" observed in superconducting resonator circuits [7] can be exploited in low phase noise hybrid oscillator design. These oscillators have the potential to replace dielectric resonator stabilized oscillators in cryogenic applications.

Several hybrid GaAs/superconducting microwave oscillators were fabricated on $1cm^2$ lanthanum aluminate substrates and tested. The design used a ring resonator in the reflection mode. A ring with a resonant frequency of 10 GHz was placed a quarter wavelength from the drain of the FET, parallel coupled to the output transmission line with a coupling gap 40 microns long. The oscillator output was taken at the drain. The best circuit had an output power of 6.4 dBm at $77K$, which corresponds to an efficiency of 10.4%. The layout of the oscillator circuit is shown in Figure 4. For the HTS circuits, the transmission lines,

rf chokes (radial stubs), and bias lines were fabricated using YBCO films, only the ground planes were fabricated in gold.

Toshiba low noise GaAs FETs (JS8830-s) were used in the design. Their S-parameters were measured from 4 to 26.5 GHz, over temperatures from $300K$ to $40K$ under a bias of $I_{ds}=10ma$ and $V_{ds}=3V$. V_{gs} was adjusted from $-1.04V$ at $300K$ to $-1.19V$ at $40K$ to maintain the desired bias condition. Of all the S-parameters measured, the magnitude of S_{21} showed the most variation over temperature, due to the increased electron mobility as the temperature was decreased. The S-parameter measurements from 15 to 26.5 GHz were unreliable due to a loss of calibration at those frequencies at the lower temperatures. This was most noticeable in the values for S_{22} . This problem has been reported before [8]. The oscillator circuit design based on the measured S-parameters at $77K$, was performed, and then optimized using Touchstone [9].

Both copper and HTS circuits were fabricated and tested for comparison purposes. They were mounted on a brass test fixture inside a closed cycle cryostat. The circuits oscillated at 10 and 20 GHz, the 20 GHz signal was 20 dB below the fundamental. The copper circuit showed little frequency sensitivity to temperature, varying about $-70 kHz/K$ from $25K$ to $100K$. The best HTS circuit showed a sensitivity of $-10 MHz/K$ in the vicinity of $77K$. This oscillator worked up to $87K$. Figure 5 plots output power vs. temperature for several circuits and Figure 6 shows output frequency vs. temperature.

The frequency of the copper circuit changed very little. The power decreased from 4.8 dBm at $25K$ to 2.8 dBm at $100K$. The efficiency of the circuit at these bias conditions at $77K$ was 4.1%.

TECHNICAL ISSUES

It should be noted that temperature cycling of devices or systems is probably the most stressful thermal condition that can be placed on them. On the other hand, operation at stable cryogenic temperatures for extended periods of time should enhance the performance of semi-conducting devices. Besides lower noise figures, cryogenic operation will in general lead to lower power consumption, longer device life due to the ease with which device power

may be dissipated, and more uniform device characteristics.

Our closed cycle cryocooler relies on a pump to achieve the desired temperature. The pump introduces a vibration into the cold finger on which the device under test (DUT) is mounted. We have found that this vibration can lead to broken external bond wires if insufficient attention is paid to layout and assembly of the DUT. Internal bonds in the packaged device appear to be unaffected. The vibration also caused instability in the HTS oscillator circuit.

CONCLUSIONS

A two-pole HTS BPF/LNA hybrid has been fully characterized at 77K and its performance compared to that of a normal metal hybrid. The hybrid showed a 2.1 dB noise figure improvement and a 0.5 dB gain improvement at 77K as compared to the gold filter/LNA hybrid. Repeated cycling over temperature showed no adverse effects on the hybrid or in the performance of the commercial LNA. There was no loss in the hermeticity of the package. Several other LNAs were also tested and similar results obtained.

The power supply to the LNA's was turned on during the entire time the hybrid was being cooled. The resulting power dissipation inside the package undoubtedly raised the temperature inside the package above 77K and prevented the nitrogen gas backfill from condensing. This was seen as a benefit since condensation of the backfill in the package could have caused short circuits. Also, the primary goal of the experiment was to integrate the HTS BPF with a commercial LNA at 77K, any further system level performance improvement due to cooling the LNA is an added benefit.

The results of superconducting oscillators were presented and their performance compared to that of similar circuits fabricated from copper. The oscillator designs were optimized for operation at 77K, rather than designed for room temperature operation and then cooled.

In deep space communications, radio astronomy and radiometer applications, low noise/low loss requirements are usually met by cooling microwave components. Long term system reliability is also critical, since there is usually no option to service the equipment once it is launched. The ability to integrate

larger systems in a cryogenic environment is contingent on reliable unattended performance. Our results on the BPF/LNA hybrid and the superconducting oscillator would indicate that reliable operation is possible without radical departures from present design techniques used for space systems.

REFERENCES

1. IEEE Trans. Microwave Theory and Tech. Special Issue on Microwave Applications of Superconductivity, vol.39, September 1991.
2. D.C. Webb and M. Nisenoff, "The High Temperature Superconductivity Space Experiment," Microwave Journal, September 1991, pp 85-91.
3. T. Van Duzer, "Superconductor-semiconductor hybrid devices, circuits and systems", Cryogenics, Vol. 28, pp.527-531, 1988
4. M.W. Pospieszalski, S. Weinreb, R.D. Norrod, and R. Harris, "FET's and HEMT's at cryogenic temperatures-their properties and use in low-noise amplifiers," IEEE Trans. Microwave Theory and Tech., Vol.36, pp.552-560, 1988.
5. S.S. Tonicich, K.B. Bhasin, T.K. Chen, and P.C. Claspy, "Performance of a wideband GaAs low noise amplifier at cryogenic temperatures" to be published in the July 1992 issue of Microwave and Optical Tech. Lett.
6. K.B. Bhasin, S.S. Tonicich, C.M. Chorey, R.R. Bonetti, and A.E. Williams, "Performance of a Y-Ba-Cu-O superconducting filter/GaAs low noise amplifier hybrid circuit," 1992 MTT-S International Microwave Symposium, Albuquerque, NM, June 2-4, 1992.
7. C.M. Chorey, K. Kong, K.B. Bhasin, J.D. Warner, and T. Itoh, "YBCO Superconducting ring resonator at millimeter wave frequencies", IEEE Trans. on Microwave Theory and Tech., Vol. 39, No. 9, p. 1480, Sept. 1991.
8. J.W. Smuk, M.G. Stubbs, and J.S. Wight, "Vector measurement of microwave device at cryogenic temperatures", IEEE Trans. Microwave Theory and Tech., Vol. MTT-S, p. 1195, 1989.
9. EEsof, Westlake Village, CA

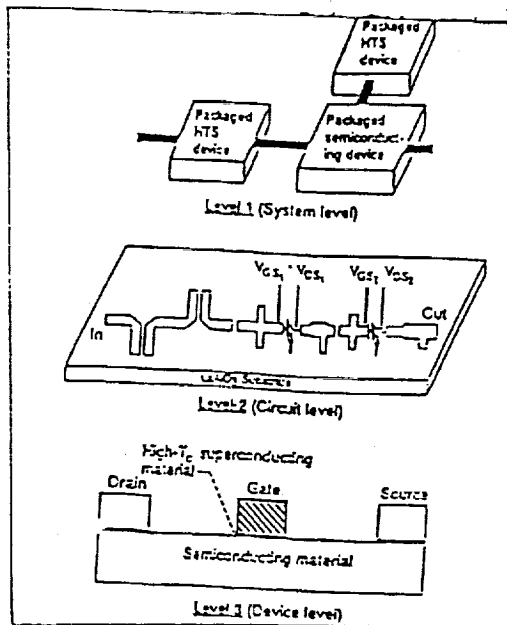
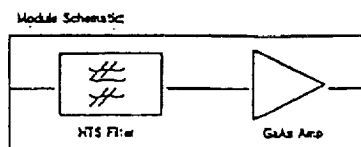


Figure 1
Possible levels of integration



MODULE PARTICULARS

- ▶ YBCO Microstrip Bandpass Filter
- ▶ Commercial GaAs Low Noise Amplifier
- ▶ Microstrip Interconnects on Duroid
- ▶ Cool Inlet and Output

Figure 2
BPF/LNA combination

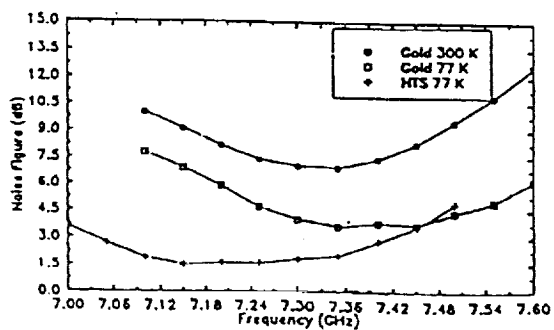


Figure 3
Noise figure for BPF/LNA combination

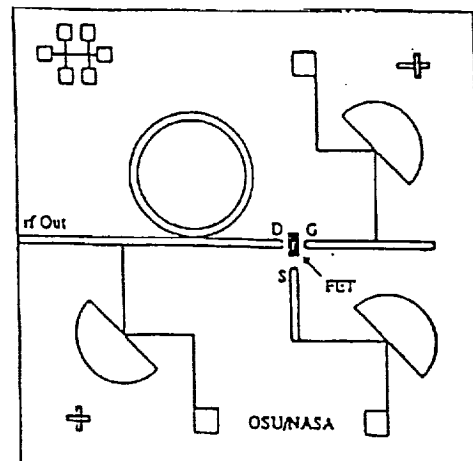


Figure 4
Oscillator layout

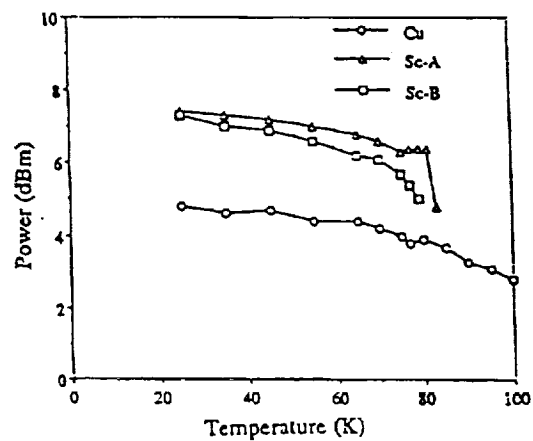


Figure 5
Output power vs. temperature

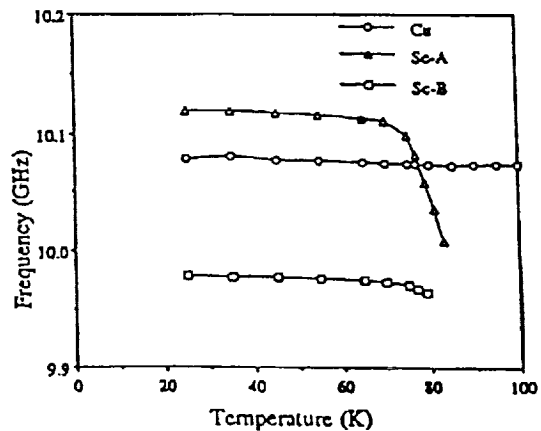


Figure 6
Output frequency vs. temperature

A HIGH TEMPERATURE SUPERCONDUCTIVITY COMMUNICATIONS FLIGHT EXPERIMENT

**P. Ngo, K. Krishen, and D. Arndt
NASA Johnson Space Center
Houston, Texas**

**G. Raffoul and V. Karasak
Lockheed
Houston, Texas**

**K. Bhasin and R. Leonard
NASA Lewis Research Center
Cleveland, Ohio**

ABSTRACT

A high-temperature superconductivity (HTSC) flight experiment from the payload bay of the Space Shuttle Orbiter to the Advanced Communications Technology Satellite (ACTS) is being breadboarded. This proposed experiment, a joint project between the Johnson Space Center and the Lewis Research Center, would use a Ka-band (20 GHz) HTSC phased array antenna and front-end electronics (low-noise amplifier) to receive a downlink communications signal from the ACTS. A conventional receiver demodulates the encoded telemetry signal which is then turned around and transmitted back to ACTS and the ground.

The HTSC phased array has nine 4 x 4 microstrip patch antenna subarrays which when properly phased, provide approximately 24 dB of boresight gain. A 2 x 2 HTSC microstrip patch has been built and tested. A Ka-band receiver, transmitter, modem, encoder, decoder, etc., are now being built and tested. Link analyses and interface problems with the Orbiter are addressed in the paper in addition to the design, fabrication, and testing of various subsystems used in the communication link.

1.0 INTRODUCTION

The recent discovery of high temperature superconductors (HTSC) has focused attention towards the search for applications that will enhance the performance of communications systems. With the natural cooling abilities of space under certain conditions, potential space applications are attractive. One application is the use of HTSC materials in microwave and millimeter-wave feed networks for large antenna arrays. This application could enhance the communications system performance primarily by reducing front-end losses, but also allowing the replacement of bulky waveguide feed structures with smaller, high performance planar structures.

This paper describes a proposed HTSC millimeter-wave communications flight experiment between a Shuttle Orbiter in low-earth-orbit and the Advanced Communications Technology Satellite (ACTS) in geosynchronous orbit. The experiment involves a Ka-band, superconducting phased array antenna with the front-end electronics developed by the Lewis Research Center (LeRC) and the receiver, with appropriate interfaces in an Orbiter's payload bay developed by Johnson Space Center personnel. Breadboard hardware for the various experiment is 1996. The advantages of such an experiment include: (1) the first use of a complete HTSC communications system operating in a manned spacecraft environment, (2) an evaluation of the thermal interfaces, cooling rates, and interfaces required for an HTSC system to work in an operational space environment, (3) provide direct distribution of data from the ground to a spacecraft without the additional hops involved in the present communication links through the Whites Sands facility, and (4) the first utilization of the 19.7 GHz forward link from the ACTS to an orbiting spacecraft.

2.0 SYSTEM CONFIGURATION

The ACTS is an experimental, geosynchronous satellite scheduled to be launched in July 1993 with a 4-year expected operational lifetime. This satellite which has been designed and developed by the LeRC, provides spot beams to fixed ground locations within the United States. It also has a 1.1 meter, computer steerable antenna which can communicate with low-earth orbiting (LEO) spacecraft. The system configuration, as shown in Figure 1, has an uplink subsystems are being built and tested. The expected time-frame for the

signal at 29.5 GHz which is transmitted from the Electronic Systems Test Laboratory at JSC or from the LeRC to the ACTS. The signal is received by the 2.2m antenna on the ACTS, routed via a matrix switch to the 1.1m antenna which transmits the signal at 19.7 GHz to the Orbiter. This is a bent-pipe mode within the ACTS with a 900 MHz IF bandwidth. The maximum Doppler shift during the experiment is approximately 500 MHz which exceeds the capability of the ACTS baseband processing mode (demodulation/modulation).

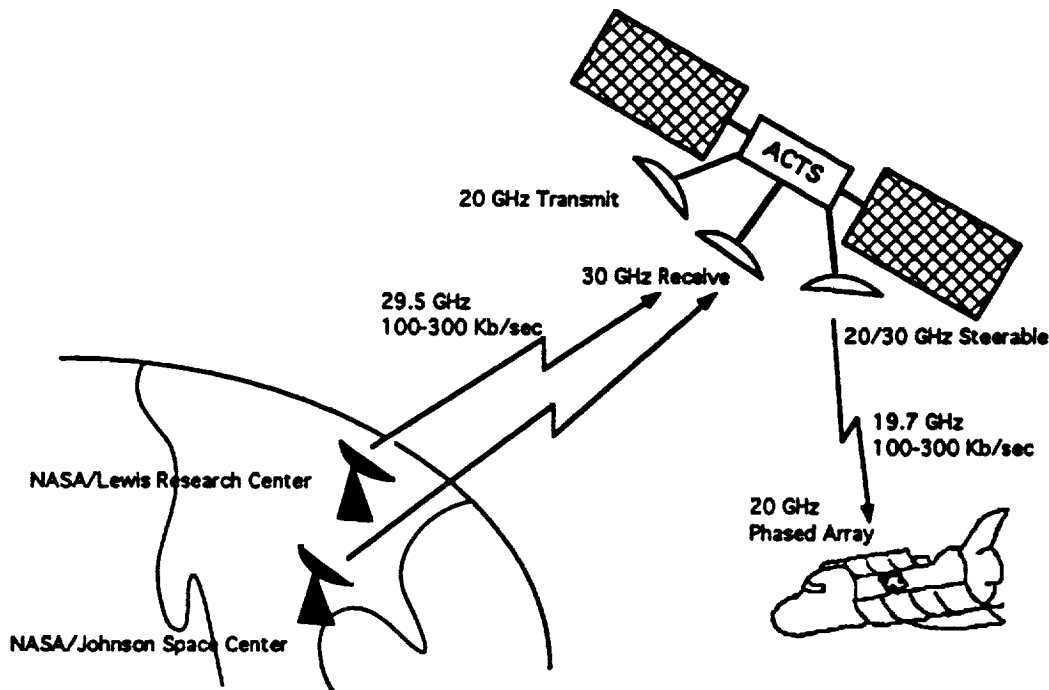


Figure 1 - ACTS 20/30 GHz Flight Experiment

The experiment program includes development of the space hardware for the Orbiter as well as ground transmitting equipment needed in the ESTL. In addition, the program includes certification testing and documentation required for flight on the Orbiter, integration into the payload bay, and the interfaces with the other Orbiter equipment. Certification testing includes four areas: thermal vacuum, vibration, structural loads, and electromagnetic interference (EMI). The experiment is categorized as a Class C payload (economically reflitable or repeatable) with no Orbiter impacts in the event of an experiment failure.

A detailed block diagram of the spacecraft equipment is given in Figure 2. The HTSC antenna could be a circular polarized phased array with nine subarrays; each subarray has 4×4 microstrip patch antennas. This antenna will be discussed in detail later in the paper. The antenna has approximately 25 dB of gain with a 10° half-power beamwidth. Each of the nine subarray feeds a low-noise amplifier (LNA), followed by a monolithic microwave integrated circuit (MMIC) phase shifter. The phase shifters are controlled by a dedicated antenna controller which takes the Orbiter's state vector available from the payload interface panel and calculates the required phase shifter settings to electronically point the beam. Mechanical pointing requirements, as determined by the 3 dB beamwidth of a subarray, is approximately $\pm 15^\circ$ for boresight alignment.

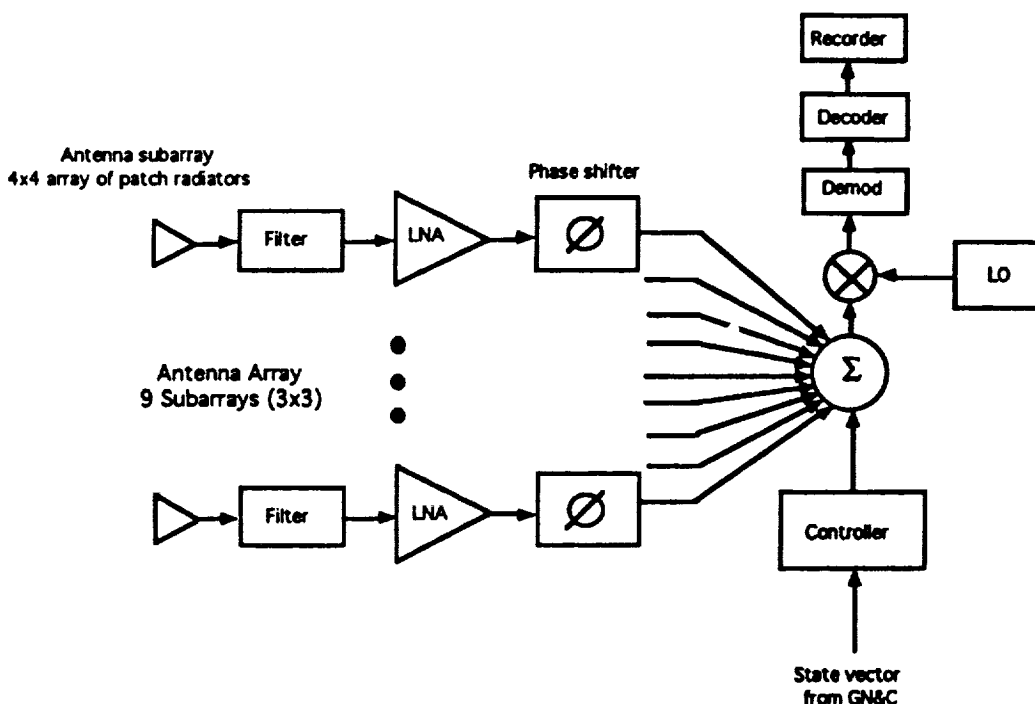


Figure 2 - Electronic Equipment Onboard the Orbiter

2.1 Ground Equipment

The ground terminal at JSC has a 1.2m parabolic antenna which is manually pointed to the ACTS. A baseband signal, 100 Kbps to 300 Kbps with convolutional encoding, is biphase modulated onto uplink carrier. The type of modulation data has not been determined.

2.2 Spacecraft Receiver

The spacecraft receiver requires either a large sweep bandwidth in order to acquire the doppler shifted signal of +/- 500 MHz with a maximum rate of change of .6 KHz/sec., or the ground transmitter must have a preprogrammed ephemeris to compensate for the doppler shift. It will probably be easier and less costly to doppler compensate on the ground. It has also not been decided whether to record the uplink data for post mission evaluation or to turn around the the data and transmit back to the ground via the normal Ku-band Tracking Data Relay Satellite System (TDRSS) link or to use the Ka-band return link of the ACTS.

3.0 LINK PERFORMANCE

The circuit margin calculations for the forward link are shown in Table 1. There is a 3 dB polarization loss in the ACTS/Orbiter link due to the linear polarized ACTS antenna and the circular polarized Orbiter antenna. The ACTS is operating in a bent-pipe configuration with a 900 MHz bandwidth; there could be signal suppression in the satellite's limiter and a power sharing loss in the output power amplifier. However, recent test data taken on a prototype ACTS system indicated little or no power sharing losses or signal suppression (private communications). Accordingly, these losses are zero in the calculations. A coding gain of 5 dB for the data is used to provide 2.9 dB of link margin for 300 Kbps of data.

4.0 THERMAL LOADING

Several thermal loading configurations were calculated for payloads located in the Orbiter's payload bay. The general equation for thermal balance is:

$$Q_{in} = Q_{out} \quad (1)$$

Solar + Earth + System Heating = Radiation to Space + Radiation to Payload
Bayliner + Conduction to Orbiter Structure

$$\alpha_s A_n Q_{solar} + \epsilon_{ir} A_n Q_{earth} + Q_{system} = \sigma \sum A_n (T_{system}^4 - T_{space}^4) + \sigma \sum A_n (T_{system}^4 - T_{liner}^4) + (kA_{cond}/l)(T_{system} - T_{beam}) \quad (2)$$

where

α_s = Solar absorptivity

A_n = area of node n

$Q_{\text{solar}} = 429 \text{ BTU/ft}^2/\text{hour}$
 ϵ_{ir} = emissitivity of infrared (dependent upon surface coating)
 $Q_{\text{earth}} = 70 \text{ BTU/ft}^2/\text{hour}$
 Q_{system} = heat dissipation in receiver (assumed 0 watts)
 σ = Stefan Boltzmann's Constant
 \mathcal{F} = view factor (percent of viewing surface area)
 T_{system} = temperature environment of HTSC component
 T_{liner} = temperature of payload bay liner
 T_{space} = temperature of outer space (0° Kelvin)
 l = length between two nodes for conduction
 T_{beam} = temperature of payload bay beam that the payload is attached to (+50° to 90°F for sun viewing, +15°F for earth viewing, and -50°F for cold space viewing)
 A_{cond} = effective cross-sectional area of conducting beam (perpendicular to payload structure)
 k = thermal conductivity of attachment beam

The analyses were performed using the Thermal Radiation Analyzer System (TRASYS) model to produce radiation conductors and heating rates for various orbit attitudes; the TRASYS output is used as an input for Systems Improved Numerical Differencing Analyzer (SINDA) model to calculate temperatures for 136 nodes (points) within the Orbiter's payload bay. Three orbital attitudes are shown in Figure 3: (1) bay to space (cold); $\text{Beta} = 90^\circ$ (polar orbit), (2) bay to sun (hot); $\text{Beta} = 90^\circ$ (polar orbit), and (3) bay to earth (warm); $\text{Beta} = 0^\circ$ (equatorial orbit).

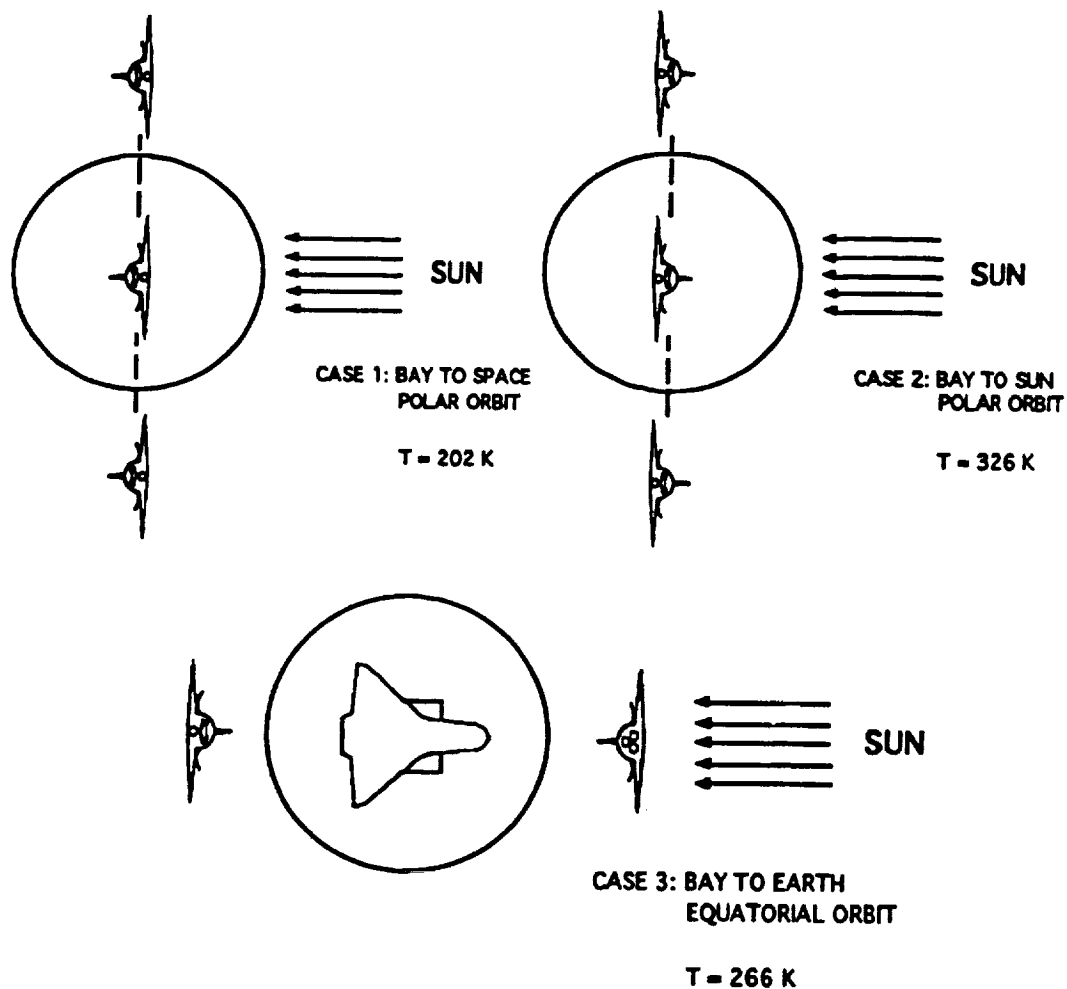


Figure 3 - Orbital Configurations for Thermal Analyses

For the earth-facing orbit, the temperature of the earth is 0°F with a heating rate of $70 \text{ BTU/ft}^2/\text{hour}$; for the sun-facing orbit, the heating rate is $429 \text{ BTU/ft}^2/\text{hour}$; for the cold (space-facing) orbit, the heating rate is $0 \text{ BTU/ft}^2/\text{hour}$. With an assumed initial temperature of 70°F , the steady-state results as shown in Figure 4 are:

Case 1 Payload bay to cold space $T = -95^{\circ}\text{F}$ (203°K)

Case 2 Payload bay to sun $T = +128^{\circ}\text{F}$

Case 3 Payload bay facing earth $T = +20^{\circ}\text{F}$

The reason for the relatively high temperature (- 95°F) in the payload bay facing cold space is due to the conduction from warmer parts of the Orbiter to the payload bay. The bottom of the Orbiter is still heated by the sun and there is a finite thermal mass within the Orbiter's structure. It is possible to achieve colder payload bay temperatures by flying in polar orbit with the bottom of the Orbiter facing the earth and the nose towards the sun.

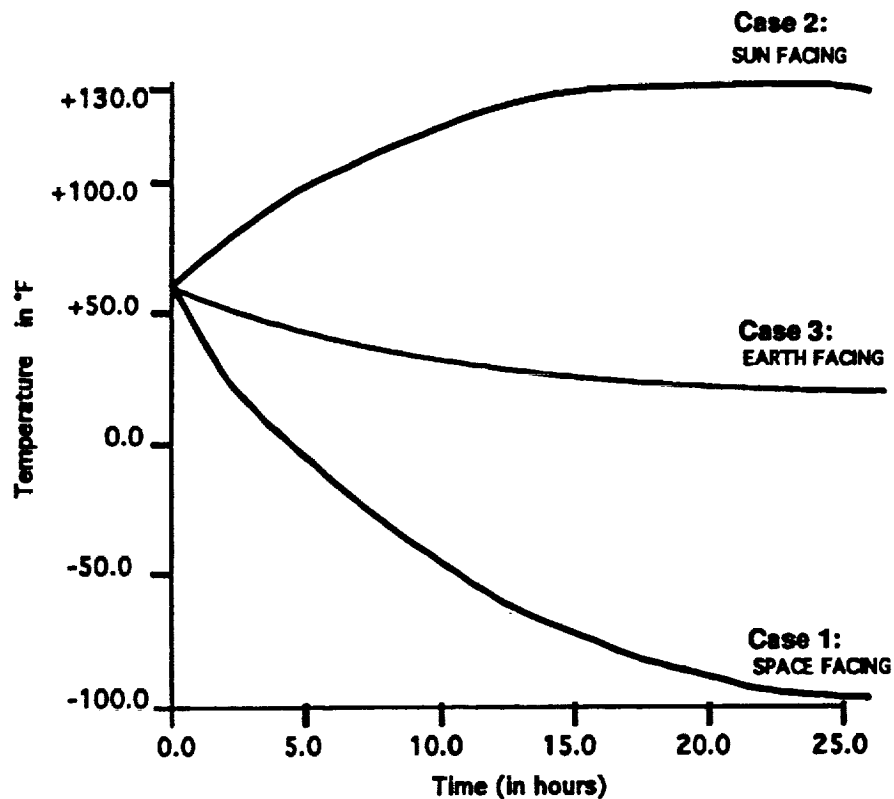


Figure 4 - Thermal Conditions in The Orbiter's Payload Bay

A payload bay temperature of - 250° F (113° K) could be achieved with even colder temperatures by using thermal isolator between the equipment and the payload bay structure. Regardless, a small cooling refrigerator will probably be necessary for the HTSC equipment.

5.0 SUPERCONDUCTING ANTENNA ARRAY

The use of HTSC materials in antenna designs will increase any antenna's radiation efficiency by reducing the ohmic losses in the structure. This appears as an increase in the gain of the antenna since gain and radiation efficiency are in direct proportion. The use of HTSC materials will have a negligible effect on the shape of the antenna's radiation pattern.

Although the gain of all normal-metal antennas can be increased to some extent via the use of superconductors, millimeter-wave arrays appear to have the greatest potential for practical improvement. For a corporate-fed array with a uniform excitation across its aperture, the gain of the array is

$$G(\text{dB}) = 10 \log(4\pi A/\lambda^2) - \alpha L \quad (3)$$

where A is the aperture area, λ is the wavelength of operation, α is the attenuation (dB/unit length), and L is the length of the transmission line from the array feed point to any radiating element. Figures 5 and 6 show how the length of the feed lines increase with increasing array size and how the feed network losses affect the gain of the array, respectively. As can be seen, if losses can be neglected ($\alpha=0$), an arbitrarily large gain can be obtained if the physical size of the array is not limited by other constraints. However, as the length of the array side increases linearly, the length of the path from the array feed point to any element increases exponentially. Eventually, any losses in the feed network become large enough to limit the maximum available gain of the structure. These calculations were done at a frequency of 20 GHz, with lossless radiating elements separated by $1/2 \lambda$. The loss value of 0.25 dB/in is typical for room-temperature CU/PTFE microstrip or stripline transmission lines at this frequency. Often, waveguide feed networks are used to reduce loss at the expense of physical size.

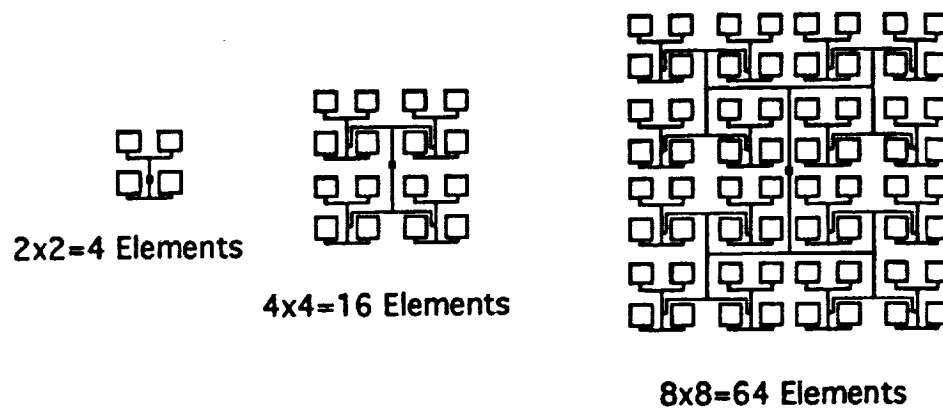


Figure 5 - Feed Network Complexity Increases Exponentially as Corporate-Fed Array Side Length Increases Linearly

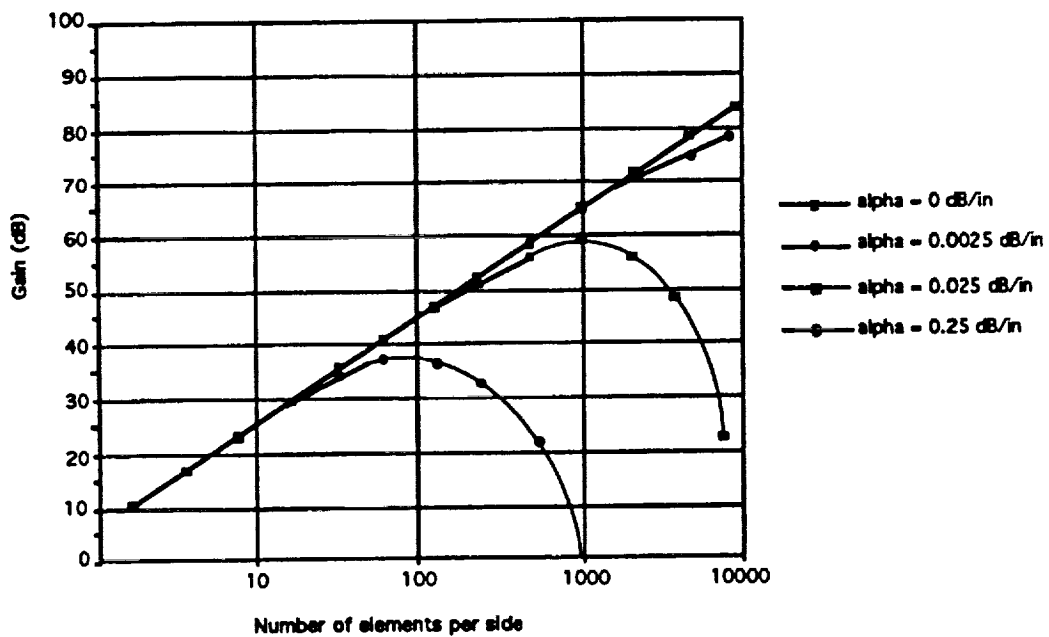


Figure 6 - Array Gain Versus Size as a Function of Feed Line Losses

Researchers at NASA/LeRC have fabricated and tested a 64-element thallium-film superconducting microstrip array operating at 30 GHz [1]. The array is fabricated on a 10 milli-inch lanthanum aluminate substrate and both the radiating elements and the microstrip corporate feed network share the same side of the substrate. At 77 K, the device has shown a 2 dB higher gain than an identical antenna pattern with gold metallization at the same temperature, and 4 dB higher gain than the room temperature gold antenna.

In the antenna described above, both the feed network and the radiating elements were fabricated from HTSC material. It is known that superconducting patch radiators show only a modest increase in efficiency over that of normal-metal designs unless the patches are fabricated on relatively thin or high-dielectric substrates [2]. In fact, microstrip patch antennas are usually fabricated on thick ($\sim \lambda_0/20$), low dielectric constant ($\epsilon_r < 10$), low-loss ($\tan\delta < 0.001$) substrates. The substrates that are presently compatible with HTSC films do not meet all these criteria. A design, presently underway at NASA/JSC, that combines a HTSC stripline feed network and normal-metal patch radiators fabricated on a relatively thick, low dielectric constant substrate is shown in Figure 7.

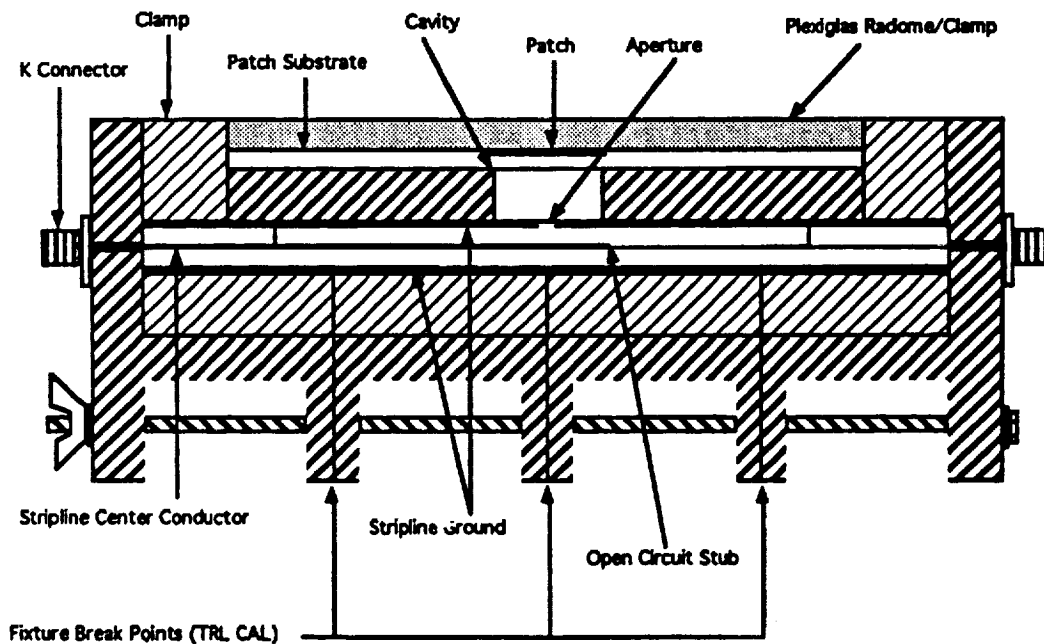


Figure 7 - Single Aperture-Coupled Patch Antenna and Test Fixture - Cross Section

Table I

ACTS-to-Orbiter Link Calculations (300 Kbps)

<u>Parameters</u>	<u>Values</u>	<u>Remarks</u>
1. ACTS transmit power, dBw	16.3	43 watts
2. ACTS transmit circuit loss, dB	-3.0	
3. ACTS transmit antenna gain, dB	42.0	1.1m antenna
4. ACTS transmit EIRP, dBw	55.3	Sum 1 thru 3
5. ACTS power sharing loss due, dB to 900 MHz bandwidth	0.0	
6. Spaceloss, dB	-210.5	40744Km, 19.7 GHz
7. Polarization loss, dB	-3.0	Linear to Circular
8. Pointing loss, dB	-.5	Estimate
9. Orbiter antenna receive, gain, dB	25.0	9 subarrays; 16 microstrip patches/sub- array
10. Orbiter receive circuit loss, dB	-0.5	HTSC lines to input LNA
11. Orbiter total receive power, dBw	-134.2	Sum 4 thru 10
12. System noise temperature, dBk	29.6	NF = 5 dB, T _a = 290°K
13. Noise spectral density (No) dB/KHz	-228.6	Boltzmann's Constant
14. Received C/No, dBHz	64.8	Lines 11 - (12 + 13)
15. Bit rate bandwidth, dBHz	54.8	300 Kbps
16. Received S/N, dB	10.0	Lines 14-15
17. Theoretical required S/N, dB	9.6	1.E-5 BER
18. Coding gain	5.0	(R = 1/2, K = 7)
19. Implementation loss, dB	-1.5	Estimate
20. Demodulation loss, dB	-1.0	Estimate
21. Required S/N, dB	7.1	Lines 17 - (18+19+20)
22. Link circuit margin, dB	2.9	Lines 16-21

6.0 REFERENCES

- [1] Lewis, L.L., Koepf, G., Bhasin, K.B., and Richard, M. A. "Performance of TlCaBaCuO 30 GHz 64 Element Antenna Array," To be presented at 1992 Applied Superconductivity Conference, Chicago.
- [2] Karasack, V.G. "High-Temperature Superconductor Antenna Investigations," *Superconductivity Applications for Infrared and Microwave Devices*, Kul B. Bhasin, Vernon O. Heinen, Editors, Proc. SPIE 1292, 93-106 (1990).

C-BAND SUPERCONDUCTOR/SEMICONDUCTOR HYBRID FIELD-EFFECT TRANSISTOR AMPLIFIER ON A LaAlO_3 SUBSTRATE

J.J. Nahra
University of Cincinnati
Cincinnati, Ohio

K.B. Bhasin and S.S. Toncich^{*}
Lewis Research Center
Cleveland, Ohio

G. Subramanyam and V.J. Kapoor
University of Cincinnati
Cincinnati, Ohio

Abstract—A single-stage C-band superconductor/semiconductor hybrid field-effect transistor (FET) amplifier was designed, fabricated, and tested at 77K. The large-area (1 inch x 0.5 inch) high temperature superconducting (HTS) Ti-Ba-Ca-Cu-O (TBCCO) thin film was rf magnetron sputtered onto a Lanthanum Aluminate (LaAlO_3) substrate. The amplifier showed a gain of 5.75 dB and a 3dB bandwidth of 150 MHz centered at 7.915 GHz at 77K. An identical gold amplifier was also tested at 77K for purposes of comparison, it had a gain of 5.46 dB centered at 7.635 GHz with a 3dB bandwidth of 100 MHz.

The objective of this work is to determine the advantage of using High T_c superconducting thin films in the input and output impedance matching networks of a GaAs FET microstrip amplifier. In deep space communications and radio astronomy where ultra low-noise amplifiers (LNA's) are very important because very weak signals need to be detected, the use of superconducting matching networks could provide for lower insertion loss, resulting in improved performance. The amplifier design, fabrication, and results are presented in the following sections.

I. INTRODUCTION

Since the discovery of high temperature superconductors (HTS) in the Thallium-Barium-Calcium-Copper-Oxide (TBCCO) and Yttrium-Barium-Calcium-Copper-Oxide (YBCO) systems [1,2], the idea of using superconductors in combination with semiconductor devices in hybrid microwave integrated circuits became feasible at liquid nitrogen temperatures [3]. Semiconductor devices such as Metal Semiconductor Field-Effect Transistors (MESFET's) and High Electron Mobility Transistors (HEMT's) have been shown to have improved device characteristics at cryogenic temperatures [4]. With the development of High T_c superconducting thin films, and Gallium Arsenide (GaAs) monolithic microwave integrated circuits high performance superconductor/semiconductor hybrid integrated circuits can now be realized. The use of superconductors and semiconductors together in microwave circuits has been demonstrated recently [5]. By combining superconducting material with semiconductor devices in microwave circuits, improved performance can be achieved in terms of decreased conductor losses, reduced noise figure (NF), and increased gain [6]. Also, by operating the amplifier at cryogenic temperatures, natural increase in gain due to increased conductivity in the transistor at low temperatures can be exploited.

II. AMPLIFIER DESIGN AND FABRICATION

A single-stage microstrip amplifier was designed for a gain of 6 dB at a center frequency of 8 GHz and a 3dB bandwidth of 500 MHz. The amplifier circuit was designed using TOUCHSTONE [7] on a Sun Workstation. For the purpose of obtaining an optimized cryogenic design the Scattering Parameters (S-Parameters) of a Toshiba GaAs transistor were measured at 77K. The S-Parameters are shown in Figure 1.

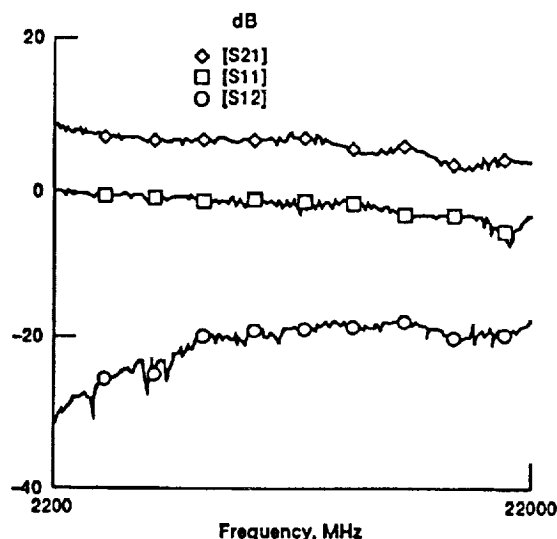


Fig. 1 S-Parameters of Toshiba GaAs FET at T = 77K

^{*}National Research Council-NASA Research Associate.

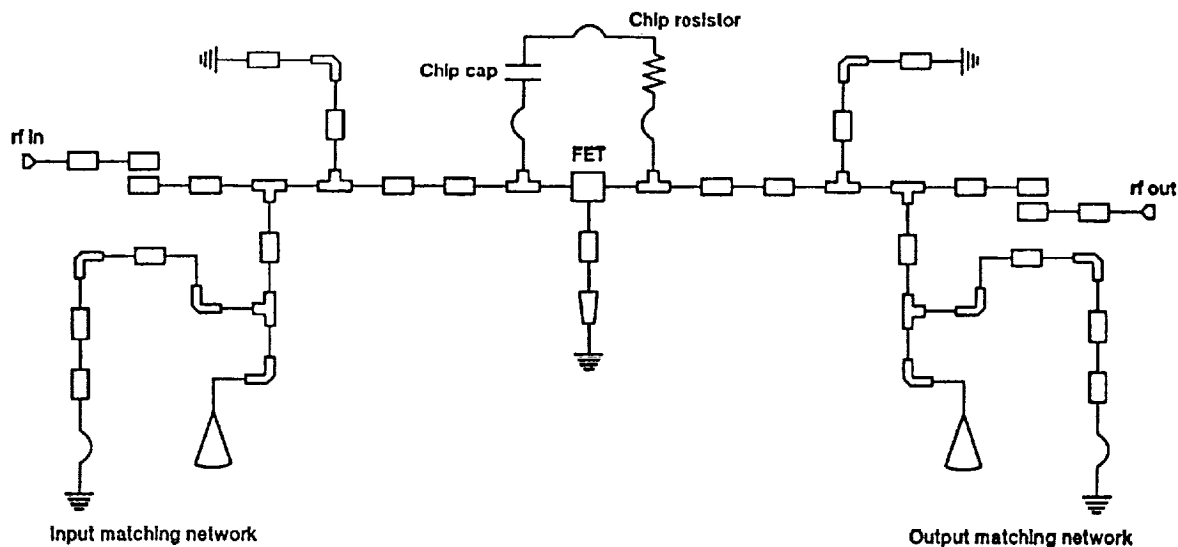


Fig. 2 Schematic of Amplifier Generated in TOUCHSTONE

The measured S-Parameter data was used to design the input and output single-stub impedance matching networks. A schematic of the design is shown in Figure 2. Input and output 50Ω feed lines are followed by coupled lines which function as dc blocks. Impedance matching was done using transmission lines of different length and width, and open-circuited shunt stubs to avoid the problem of fabricating high quality wide band short circuits. The grounding of the source terminal of the transistor was performed by using a low impedance transmission line terminated in a low impedance tapered line. The end of the tapered line came to the edge of the substrate and silver paint was applied to this edge in order to provide an rf ground path to the test fixture.

The amplifier matching and dc bias networks were fabricated by rf magnetron sputtering a TBCCO film from a single composite powder target of $Tl_2Ba_2Ca_2Cu_3O_x$ to a thickness of 3750 \AA onto a 20 mil thick $LaAlO_3$ substrate [8]. Gold contact areas for wire bonding purposes were formed through a lift-off process and $2.5\mu\text{m}$ of silver was thermally evaporated on the opposite side of the substrate which acted as the ground plane. A Toshiba GaAs FET was mounted on the substrate using silver-filled conductive epoxy and cured at 150°C for 1 hour. A feedback network consisting of a chip resistor and chip capacitor was added to the amplifier design in order to ensure stability because the amplifier had a tendency to oscillate. The FET, chip capacitor, and chip resistor were connected to the appropriate microstrip lines with 0.7 mil diameter gold bond wires. The amplifier was mounted in a brass test fixture inside a cryogenic chamber on a cold-head platform. Inside the chamber semi-rigid coaxial lines connected the input and output ports of the amplifier to the outside of the cryogenic chamber. Input and output 3.5mm SMA female connectors provided a coax to

microstrip feed line transition. Silver paint was used to ensure electrical contact between the launcher pin and the microstrip line. A photograph of the amplifier in its test fixture is shown in Figure 3. An identical amplifier using gold film for the microstrip lines and ground plane was also fabricated for use as a comparison to the hybrid amplifier.

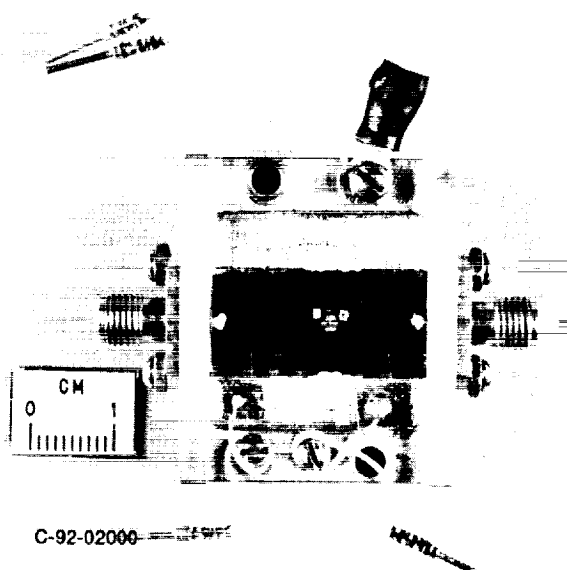


Fig. 3 Photograph of Hybrid Amplifier in Test Fixture

III. MEASUREMENTS AND RESULTS

An HP8510B Vector Network Analyzer and a model 22C Cryodyne closed-cycle refrigeration system made by CTI-

Cryogenics were used to measure the S-Parameters of the amplifiers at 77K. The amplifier was mounted in the cryogenic chamber and the semi-rigid coaxial lines were connected to the input and output ports respectively. The chamber was evacuated to 50 milli torr and the transistor dc bias was applied. The corresponding S-Parameters were measured and recorded. The forward gain of the hybrid and gold amplifiers are shown in Figures 4 and 5 respectively.

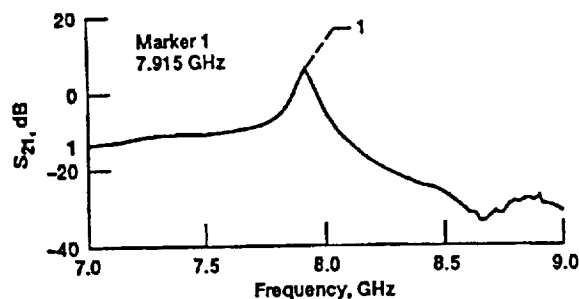


Fig. 4 Measured Gain of Hybrid Amplifier at T = 77K

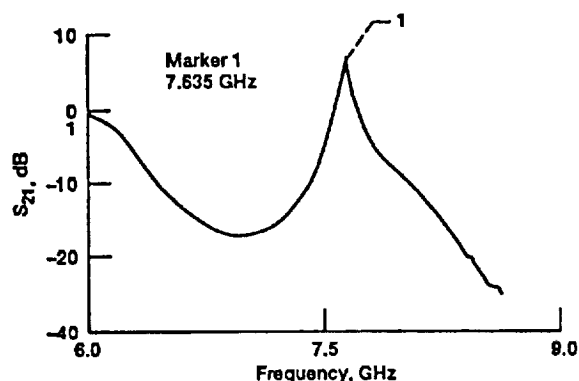


Fig. 5 Measured Gain of Gold Amplifier at T = 77K

The primary advantage of using TBCCO matching networks instead of gold is that the conductor losses are decreased and the NF can also be reduced. Since the superconducting material reacts differently than gold in terms of impedance one must design the matching networks taking into account in the simulation the properties of the superconducting material (i.e. surface resistance, thickness, and film uniformity) as compared to the properties of the gold film.

A comparison of the results obtained for the hybrid amplifier and the gold amplifier are shown in Table 1. Even though the results of the two circuits are not exactly comparable because of the differences in the impedance of the two materials it can be seen from Table 1 that the hybrid amplifier results were closer to the original design goals. This is because the properties of the superconducting material, such as thickness and resistivity, were taken into account in the design.

IV. CONCLUSIONS

A single-stage TBCCO/GaAs FET amplifier was fabricated and its S-Parameters were measured at 77K. An identical gold film amplifier was also fabricated and characterized at 77K. The hybrid amplifier showed a gain of 5.75 dB at a center frequency of 7.915 GHz while the gold amplifier showed a gain of 5.46 dB at a center frequency of 7.635 GHz. The hybrid amplifier was 1.0 inches long and 0.5 inches wide.

ACKNOWLEDGMENTS

This work was performed under a grant from NASA Lewis Research Center, grant number NCC3-33.

REFERENCES

- [1] M.K. Wu, J.R. Ashburn, and C.J. Torng, "Superconductivity at 93K in a New Mixed-Phase Y-Ba-Cu-O Compound System at Ambient Pressure", *Physical Review Letters*, vol. 58, No.9, pp. 908-910, March 2, 1987.
- [2] Z.Z. Sheng and A.M. Herman, "bulk Superconductivity at 120K in the Tl-Ca/Ba-Cu-O System", *Nature*, vol. 332, pp. 138-139, March 10, 1988.
- [3] T. Van Duzer, "Superconductor - Semiconductor Hybrid Devices, Circuits and Systems", *Cryogenics*, vol. 28, pp. 527-531, August 1988.
- [4] M.W. Pospieszalski, S. Weinreb, R.D. Norrod, and R. Harris, "FET's and HEMT's at Cryogenic Temperatures - Their Properties and Use in Low-Noise Amplifiers", *IEEE Transactions on Microwave Theory and Techniques*, vol. 36, No. 3, pp. 552-560, March 1988.

Table 1. Comparisons of Results of Hybrid and Gold Amplifiers at 77K

Amplifier Type	Gain (dB)	Center Frequency (GHz)	3dB Bandwidth (MHz)
Hybrid, T=77K	5.75	7.915	150
Gold, T=77K	5.46	7.635	100

[5] K.B. Bhasin, S.S. Toncich, C.M. Chorey, R.R. Bonetti, A.E. Williams, "Performance of a Y-Ba-Cu-O Superconducting Filter/GaAs Low Noise Amplifier Hybrid Circuit", IEEE Microwave Theory and Techniques International Microwave Symposium Digest, vol. 1, pp. 481-483, 1992.

[6] T. Van Duzer, "Superconductor Electronics", Cryogenics, vol. 30, pp. 980-995, December 1990.

[7] EESOF, Inc., Westlake Village, CA, 1992.

[8] G. Subramanyam, F. Radpour, V.K. Kapoor, "Fabrication of Tl-Ca-Ba-Cu-O Superconducting Thin Films on LaAlO_3 Substrates", Applied Physics Letters, vol. 56, pp. 1799-1801, 30 April 1990.